

# Shear-Rate Dependent Surface Tension of Glass-Forming Fluids

Linnea Heitmeier and Thomas Voigtmann\*

*Institut für Materialphysik im Weltraum, Deutsches Zentrum für Luft- und Raumfahrt (DLR) e.V. 51170 Köln, Germany and Heinrich-Heine-Universität Düsseldorf Universitätsstraße 1 40225 Düsseldorf, Germany*

(Dated: March 12, 2025)

We investigate the interface of a glass-forming fluid showing non-Newtonian rheology. By applying shear flow in the interface, we detect that the surface tension depends on the shear rate. Importantly, the standard way of determining surface tension from the pressure drop across the interface gives rise to an effective surface tension in the non-Newtonian fluid that mixes bulk and interface properties. We show how the pressure anisotropy can be used to clearly define the bulk and interface regions and extract a genuine shear-rate dependent surface tension. The results have implications for measurement techniques related to interfacial rheology of complex fluids.

The surface of glass-forming fluids is home to many intriguing dynamical phenomena. In an analogy to surface melting, the physical mechanism conjectured to facilitate ice skating at low temperatures, glasses are covered by layers of enhanced molecular mobility [1, 2]. The highly mobile layers near the surface facilitate the fabrication by layerwise deposition of ultrastable glasses with unique mechanical properties [3–5], and are a major factor in determining the properties of polymer films [6]. The surface induces a dynamical penetration depth into the bulk that changes non-monotonically with temperature and allows to disentangle the change in mechanisms of relaxation close to a dynamical cross-over temperature  $T_c$  [7].

Surface tension is a key parameter characterizing interfaces of complex fluids [8], but not many theoretical studies address it in the dynamical cross-over regime close to the kinetic arrest transition. This is despite the significance in applications for films and coatings, in interfacial rheology in general [9], for certain 3d-printing techniques [10], and also for theoretical concerns: The surface tension of amorphous structures in contact with each other is posited by some theories to play a key role in the dynamical cross-over from supercooled liquid to glass [11, 12].

Glass formers typically are shear-thinning and yield-stress fluids, i.e., their viscosity strongly decreases with the flow rate, and they flow only above a certain threshold stress close to  $T_c$  as the structural relaxation rate of the quiescent fluid drops below the imposed flow rate [13, 14]. Reliable experimental data for the surface tension of such non-Newtonian fluids are rare, since the emerging yield stress impedes measurements [15]. Due to the associated slow relaxation time scale of the fluid, typical measurements [15, 16] are prone to hysteresis effects. For example, Jørgensen *et al.* [15] used a liquid-bridge tensionmeter and found the apparent surface tension of carbopol dispersions to be systematically higher in expansion than in compression. They rationalized this finding with an elastoplastic model of the fluid, and attributed it to the existence of a yield stress.

This poses a number of questions: first, how does the surface tension, a parameter that is typically considered given by the “static” pressure difference across the inter-

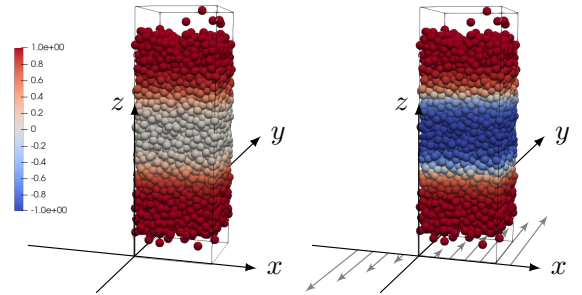


FIG. 1. Snapshots of the simulation setup without (left) and with (right) imposed shear. Only the central part of the box along  $z$  is shown for clarity. We impose ‘in-plane’ shear, as shown by the arrows in the coordinate system. Particles are colored according to  $\Delta p = p_z - (p_x + p_y)/2$  normalized to the interval  $[-1, 1]$ , see Fig. 3.

face (see below), couple to the non-Newtonian rheology of highly viscoelastic fluids, a typical “dynamic” effect in the bulk? Second, since the bulk rheology of the shear-thinning fluid depends very sensitively on the shear rate, what is the effect of fluid flow on the (apparent) surface tension?

We address these questions by molecular dynamics (MD) simulations of a prototypical model of a glass-forming fluid (involving no polymeric or suspension effects), in a simple setup involving a planar surface. Our simulations reveal how an apparent surface tension arises in non-Newtonian fluids that is a mixture of genuine surface effects, and a bulk effect.

We consider the standard Kob-Andersen binary Lennard-Jones (LJ) mixture [17] at fixed number density  $\rho = 1.2$  using the open-source package LAMMPS [18]. Units of length,  $\sigma$ , time,  $\tau_0$ , and energy are all in standard LJ units related to the larger particles. The simulations start from bulk liquids in the  $NVT$  ensemble, that are equilibrated at  $T_i = 2.0$  for at least  $500\tau_0$ , cooled to the target temperature  $T$ , and then equilibrated again for up to  $10^6\tau_0$  (depending on  $T$ ). We use  $N = 5000$  ( $N = 10000$ ) particles corresponding to a cubic box of size  $L = L_x = L_y = 13\sigma$  and  $L_z = 24.6\sigma$  ( $49.2\sigma$ ) for the small (large) system. For the determination of the

surface tension from capillary theory, alongside the small system, a wide system with  $L = 18\sigma$  with  $N = 9564$  particles was used.

After equilibration, the simulation box is enlarged to  $L_z = 160\sigma$  keeping the fluid in the center of the box such that around  $z = 0$ , bulk properties are recovered [7]. The interfaces were then relaxed for  $250\tau_0$ , before measurements were performed. Shear flow with rate  $\dot{\gamma}$  is imposed in the  $(x, y)$ -plane tangential to the surface (see Fig. 1) using the SLLOD equations; this is also motivated by the tangential character of the surface tension [19–22]. Surface tension values were averaged over at least  $2000\tau_0$ . Inspection of the  $z$ -dependent density profiles revealed no particle-species segregation.

We use two independent methods to determine the surface tension  $\hat{\sigma}$ : first from the pressure difference as suggested by equilibrium statistical physics [23],

$$\hat{\sigma} = \frac{1}{2} \int dz \left[ p_z(z) - \frac{1}{2} (p_x(z) + p_y(z)) \right], \quad (1)$$

where the integral extends from the bulk of one phase (the vapor) to the other (the fluid). A factor of  $1/2$  is included due to the second interface. Note that convergence of this integral assumes the integrand to vanish at sufficiently large  $|z|$ , which is the case in the isotropic Newtonian fluid. Essentially we argue that this integral has to be taken with care in the case of a non-Newtonian fluid with shear.

To cross-check our results, we make use of the relation between surface tension and the width of the density profile  $\Delta$  [24–26]:

$$\Delta^2 = \Delta_0^2 + \frac{k_B T}{2\pi \cdot \hat{\sigma}} \cdot \ln(L/B_0), \quad (2a)$$

where we fit the density profile according to

$$\rho(z) = \frac{\rho_l}{2} - \frac{\rho_l}{2} \cdot \tanh\left(\frac{2 \cdot (z - z_0)}{\Delta}\right), \quad (2b)$$

with the bulk liquid density  $\rho_l$ , and  $z_0$  a fit parameter for the position of the interface. In Eq. (2a),  $\Delta_0$  and  $B_0$  are unknown prefactors determined from fits for two different  $L$  (small and wide system).

We checked that our results recover the surface-tension values for the one-component quiescent LJ fluid reported in Ref. [27]. For reference, the bulk viscosity was determined using the standard Green-Kubo relation [28] in simulations of the bulk fluid, using a correlation time of up to  $100\tau_0$ .

We begin by summarizing the temperature dependence in the quiescent system. As the glass transition is approached, the viscosity of the bulk fluid strongly increases; for around two orders of magnitude in the interval  $T = [0.5, 1]$  studied here (stars in Fig. 2). The data is in the regime of the mode-coupling theory of the

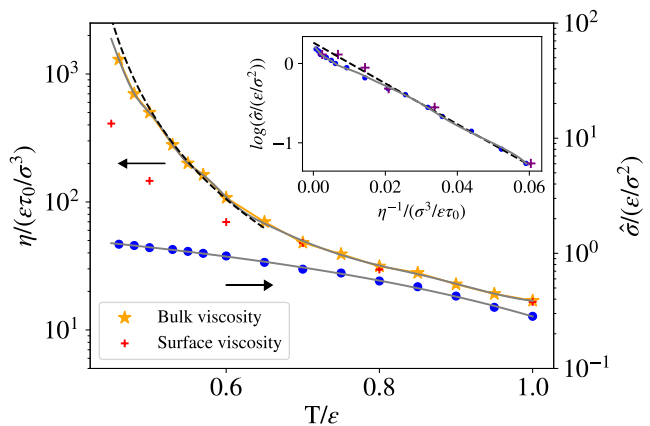


FIG. 2. Bulk viscosity (star symbols) and surface tension (circles) of the quiescent system as function of inverse temperature. Solid lines are guides to the eye. A dashed line indicates the power-law predicted by mode-coupling theory, and crosses indicate the surface viscosity (see text). Inset: logarithm of the surface tension as a function of inverse viscosity (circles) and inverse surface viscosity (crosses).

glass transition (MCT): close to the cross-over temperature  $T_c$  of MCT, the viscosity shows power-law growth,  $\eta \sim |T - T_c|^{-\gamma}$  from which deviations would set in at lower temperatures (a dashed line in Fig. 2 indicates the power law with  $T_c = 0.4$  and  $\gamma = 2.35$ ). In the same temperature interval, the surface tension (circles) increases by almost a factor of 4. Notably, it initially increases alongside the viscosity in the regime of temperatures  $T \gtrsim 0.5$ , while at lower temperatures it decouples and appears to saturate. Such saturation is in line with the interpretation that the surface tension is a “static” fluid property rather than a dynamical one coupled to the slow relaxation mechanisms captured in MCT.

It has been stated that surface tension and viscosity can be related: the empirical relation  $\ln(\hat{\sigma}) = \ln(A) + B/\eta$  was proposed [29, 30], with coefficients  $A$  and  $B$  determined from fits. This relation holds reasonably well in the not-too-viscous regime ( $\eta \lesssim 50$ ; inset of Fig. 2). For higher viscosities, we see deviations that we attribute to the slow structural relaxation affecting the viscosity.

Particles close to the surface of a glass-forming fluid retain higher mobility than in the bulk [1, 2, 31]. It hence suggests itself to define a “surface viscosity” that might bear a closer connection to the surface tension since it will grow less strongly than the bulk viscosity.

We have determined the surface viscosity by constraining the Green-Kubo integral to particles starting in  $z$ -layers close to the surface. The notion of “close” can be made precise by looking at the normal-stress differences,  $\Delta p_{\alpha\beta} = p_\alpha - p_\beta$ , where  $\alpha\beta \in \{x, y, z\}$ . Recall that in the isotropic bulk, all  $\Delta p_{\alpha\beta} = 0$ . Close to the surface, the values for  $\beta = z$ ,  $\alpha \in \{x, y\}$ , deviate from zero since the surface induces an anisotropy. This allows to

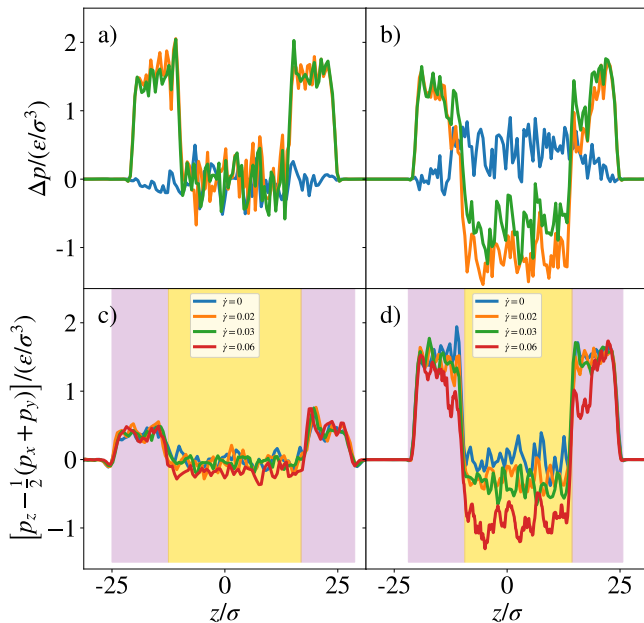


FIG. 3. Pressure differences across the interface: Top panels show  $\Delta p_{\alpha\beta} = p_\alpha - p_\beta$  (blue:  $\Delta p_{xy}$ ; green:  $\Delta p_{xz}$ ; orange:  $\Delta p_{yz}$ ) for temperature  $T = 0.6$  in (a) the quiescent system and (b) with shear rate  $\dot{\gamma} = 0.06$ . Bottom panels show the relevant pressure difference for the surface tension,  $-(\Delta p_{xz} + \Delta p_{yz})/2$ , for (c) temperature  $T = 1$ , and (d)  $T = 0.6$ . Color shadings indicate the  $z$ -intervals identified as bulk and surface regions.

clearly distinguish a surface layer (top panels in Fig. 3). This surface layer somewhat broadens upon decreasing temperature, consistent with the existence of a growing length scale near the glass transition [7]. We note in passing that the thus identified surface layer to define a surface viscosity (crosses in Fig. 2), indeed follows the empirical relation to the surface tension more closely, although approaching to  $T_c$  it still appears to break down.

Now we turn to surfaces with in-plane shear flow. Glass formers are non-Newtonian fluids, featuring non-vanishing normal-stress differences in the bulk. Recall that we apply a velocity in the  $y$ -direction, with gradient in the  $x$ -direction; thus the first and second bulk normal stress differences are given by [32]  $N_1 = \sigma_{yy} - \sigma_{xx}$  and  $N_2 = \sigma_{xx} - \sigma_{zz}$ , where  $\sigma_{\alpha\alpha} = -p_\alpha$ . The Kob-Andersen system indeed shows  $N_1 = \Delta p_{xy} > 0$  and  $N_2 = -\Delta p_{xz} > 0$  with  $|N_2| \approx N_1$  (Fig. 3b, middle section).

Crucially, the surface-near region remains different: here, pressure differences are related to the surface tension, and separate from the bulk. The changes in these regions will be related to a change in surface tension under shear. They become more pronounced at lower temperatures, as  $T_c$  is approached, while at higher temperatures the effect vanishes (lower panels of Fig. 3).

However, the bulk values give non-trivial contributions

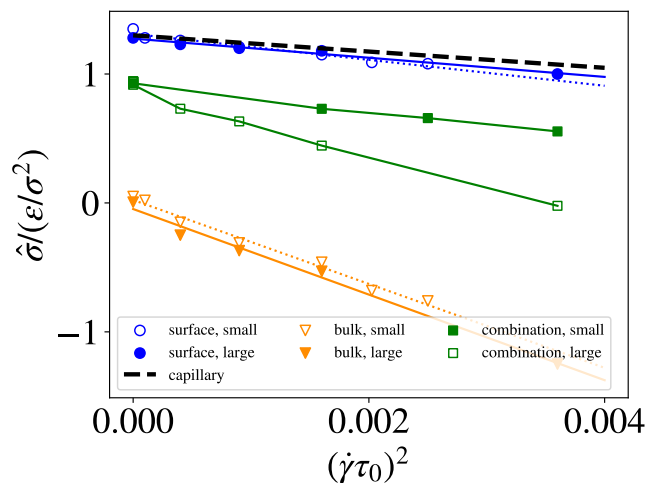


FIG. 4. Shear-rate dependence of the surface tension, as a function of the square shear rate  $\dot{\gamma}^2$ , for the Kob-Andersen mixture at  $T = 0.6$ . Blue symbols show values extracted from the pressure difference, a dashed line the trend extracted from capillary wave analysis. The contribution from the bulk of the non-Newtonian fluid (orange) leads to a system-size dependent effective surface tension (green), if evaluated by the pressure difference.

to the surface-tension integral that are specific to non-Newtonian fluids, and need to be taken into account when determining the surface tension of the sheared fluid. Also this effect becomes more pronounced when temperature is lowered: At  $T = 1$ , the fluid is nearly Newtonian, identified by vanishing normal-stress differences in the bulk (Fig. 3c); here we observe that also the dependence of the pressure anisotropy in the surface region on the shear rate is negligible. But at  $T = 0.6$ , the non-Newtonian effects are already pronounced: with increasing shear rates, increasing bulk normal-stress differences are seen; also the surface regions begin to show a shear rate dependence (Fig. 3d). In Eq. (1), hence an increasing bulk contribution is present the leads to an apparent surface tension in the non-Newtonian fluid.

The two regions in  $z$  – the surface layer identified by positive  $\Delta p_{\alpha z}$ , and the bulk liquid where these quantities have opposite sign – give rise to two different contributions to the surface-tension integral (blue and orange symbols in Fig. 4). Both depend quadratically on the shear rate, as is expected from the symmetry of the problem under reversal of the flow direction.

Intuitively, it is the pressure drop across the surface layer that relates to the surface properties. We confirm this by determining the surface tension from an analysis of the density profile, Eq. (2). Since this procedure determines  $\hat{\sigma}$  only up to a prefactor, we have adjusted this to match the value obtained from Eq. (1) at zero shear rate. The results for the  $\dot{\gamma}$ -dependence then are in very good agreement with each other (dashed black line in Fig. 4).

One notes that the bulk contribution to the pressure anisotropy is much stronger in the non-Newtonian fluid than close to the surface; hence the overall apparent surface tension in the thin film has a stronger shear-rate dependence than the actual surface tension. It also demonstrates a pronounced system-size effect (green symbols in Fig. 4). Larger systems are more strongly influenced by the non-Newtonian bulk rheology, to the point that the apparent surface tension might even vanish at large shear rates. It should be noted that this is not a destabilization of the interface; it is rather a non-equilibrium signature of the driven system, similar to what has been observed in active fluids [33, 34].

Note that in our simulations we observe the surface tension to relax to its stationary value after application of the shear flow very rapidly; in particular, we observe this process to be much faster than the structural relaxation time in the bulk. This further underlines that the mobile surface layers decouple from the slow dynamics of the bulk, but their shear-rate dependence still represents an intriguing coupling between bulk and surface dynamics.

In summary, we have shown that the surface tension of a typical glass-forming viscoelastic fluid shows a strong shear-rate dependence. In non-Newtonian fluids, normal-stress differences in the bulk and surface anisotropy of the stress tensor conspire to an *effective surface tension* that is measured using standard techniques that are based on the pressure drop across a liquid film and mix two different contributions. One contribution is a genuine surface contribution, and it comes from the pressure anisotropy in the layers near the surface. In the simulation they can be clearly identified through the different sign of  $\Delta p_{\alpha z}$  with respect to the bulk. In addition, there is a non-trivial bulk contribution arising from non-vanishing normal-stress differences, a typical non-Newtonian fluid effect.

This effect might explain why the determination of surface tension values from pressure balances of bulk viscoelastic samples is difficult, as in experiment it will be difficult to disentangle the pure surface from a bulk contribution. Also, hysteresis effects as previously reported might be arising from a non-Newtonian bulk contribution: we have monitored the transient evolution of the pressure differences after switching on the shear flow, and found no sign of slow relaxation in the surface contribution. But the bulk quantities are known to exhibit patterns of slow relaxation. Also, a changing volume-to-surface ratio, as in techniques where a fluid droplet is expanded or compresses, might see effects from different mixing of surface and bulk contributions.

Our findings should be relevant to a growing number of techniques measuring interfacial rheological properties in films of complex fluids and even for the printability of bio-inks in surface-tension assisted 3d-printing techniques [35]. For example, biofilms are known to exhibit complex rheology, and characterization of their mechan-

ical surface properties is an important aspect in their growth and removal [36, 37]. The complex interactions in such films can render the surface tension anisotropic [9], and our method of imposing in-plane shear flow in different directions might be a straight-forward way to interrogate the characteristics of the interface in such cases.

On a more theoretical note, it has been shown that the surface of glass-forming fluids reveals non-monotonic changes in the dynamical correlation length governing glassy dynamics [1, 7]. However, this analysis was only based on local density profiles and  $z$ -resolved density correlation functions. In principle, the discussion of pressure differences as done in our work should give a more natural handle on disentangling surface-induced from bulk effects in such systems. Also, we leave for further discussion the fate of the surface tension in the deeply supercooled regime (below the MCT transition).

We acknowledge fruitful discussions with N. J. Wagner and O. D'Angelo. The authors gratefully acknowledge the scientific support and HPC resources provided by the German Aerospace Center (DLR). The HPC system CARO is partially funded by "Ministry of Science and Culture of Lower Saxony" and "Federal Ministry for Economic Affairs and Climate Action".

---

\* thomas.voigtmann@dlr.de

- [1] L. Tian and C. Bechinger, Surface melting of a colloidal glass, *Nature Commun.* **13**, 6605 (2022).
- [2] P. Zhang, J. J. Maldonis, Z. Liu, J. Schroers, and P. M. Voyles, Spatially heterogeneous dynamics in a metallic glass forming liquid imaged by electron correlation microscopy, *Nature Commun.* **9**, 1129 (2018).
- [3] S. F. Swallen, K. L. Kearns, M. K. Mapes, Y. S. Kim, R. J. McMahon, M. D. Ediger, T. Wu, L. Yu, and S. Satija, Organic glasses with exceptional thermodynamic and kinetic stability, *Science* **315**, 353 (2007).
- [4] L. Berthier, P. Charbonneau, E. Flenner, and F. Zamponi, Origin of ultrastability in vapor-deposited glasses, *Phys. Rev. Lett.* **119**, 188002 (2017).
- [5] C. Rodriguez-Tinoco, M. Gonzalez-Silveira, M. A. Ramos, and J. Rodriguez-Viejo, Ultrastable glasses: new perspectives for an old problem, *Nuovo Cimento* **45**, 325 (2022).
- [6] M. D. Ediger and J. A. Forrest, Dynamics near free surfaces and the glass transition in thin polymer films: A view to the future, *Macromolecules* **47**, 471 (2014).
- [7] H. Peng, H. Liu, and T. Voigtmann, Nonmonotonic dynamical correlations beneath the surface of glass-forming liquids, *Physical Review Letters* **129**, 215501 (2022).
- [8] G. G. Fuller and J. Vermant, Complex fluid-fluid interfaces: Rheology and structure, *Annu. Rev. Chem. Biomol. Eng.* **3**, 519 (2012).
- [9] N. O. Jaensson, P. D. Anderson, and J. Vermant, Computational interfacial rheology, *J. Non-Newt. Fluid Mech.* **290**, 104507 (2021).
- [10] H. Ragelle, M. W. Tibbitt, S.-Y. Wu, M. A. Castillo, G. Z. Cheng, S. P. Gangadharan, D. G. Anderson, M. J.

- Cima, and R. Langer, Surface tension-assisted additive manufacturing, *Nature Commun.* **9**, 1184 (2018).
- [11] C. Cammarota, A. Cavagna, G. Gradenigo, T. S. Grigera, and P. Verrocchio, Evidence for a spinodal limit of amorphous excitations in glassy systems, *J. Stat. Mech.*, L12002 (2009).
- [12] D. Ganapathi, K. H. Nagamanasa, A. K. Sood, and R. Ganapathy, Measurements of growing surface tension of amorphous-amorphous interfaces on approaching the colloidal glass transition, *Nature Commun.* **9**, 397 (2018).
- [13] T. Voigtmann, Nonlinear glassy rheology, *Curr. Opin. Colloid Interf. Sci.* **19**, 549 (2014).
- [14] N. J. Wagner and J. Mewis, eds., *Theory and Applications of Colloidal Suspension Rheology* (Cambridge University Press, Cambridge, UK, 2021).
- [15] L. Jørgensen, M. Le Merrer, H. Delanoë-Ayari, and C. Barentin, Yield stress and elasticity influence on surface tension measurements, *Soft Matter* **11**, 5111 (2015).
- [16] J. Boujlel and P. Coussot, Measuring the surface tension of yield stress fluids, *Soft Matter* **9**, 5898 (2013).
- [17] W. Kob and H. C. Andersen, Testing mode-coupling theory for a supercooled binary lennard-jones mixture. ii. intermediate scattering function and dynamic susceptibility, *Physical Review E* **52**, 4134 (1995).
- [18] S. Plimpton, Fast parallel algorithms for short-range molecular dynamics, *Journal of computational physics* **117**, 1 (1995).
- [19] G. Navascues, Liquid surfaces: theory of surface tension, *Reports on Progress in Physics* **42**, 1131 (1979).
- [20] K. Birdi, *Surface tension and interfacial tension of liquids* (CRC: New York, 1997).
- [21] P.-G. Gennes, F. Brochard-Wyart, D. Quéré, *et al.*, *Capillarity and wetting phenomena: drops, bubbles, pearls, waves* (Springer, 2004).
- [22] M. Durand, Mechanical approach to surface tension and capillary phenomena, *American Journal of Physics* **89**, 261 (2021).
- [23] J. S. Rowlinson and B. Widom, *Molecular Theory of Capillarity* (Dover, New York, 1982).
- [24] R. Evans, The nature of the liquid-vapour interface and other topics in the statistical mechanics of non-uniform, classical fluids, *Advances in physics* **28**, 143 (1979).
- [25] S. W. Sides, G. S. Grest, and M.-D. Lacasse, Capillary waves at liquid-vapor interfaces: A molecular dynamics simulation, *Physical Review E* **60**, 6708 (1999).
- [26] R. Vink, J. Horbach, and K. Binder, Capillary waves in a colloid-polymer interface, *The Journal of chemical physics* **122** (2005).
- [27] J. F. Lutsko and C. Schoonen, Classical density-functional theory applied to the solid state, *Physical Review E* **102**, 062136 (2020).
- [28] D. J Evans and G. P Morriss, *Statistical mechanics of nonequilibrium liquids* (ANU Press, 2007).
- [29] A. H. Pelofsky, Surface tension-viscosity relation for liquids., *Journal of Chemical and Engineering Data* **11**, 394 (1966).
- [30] G. Di Nicola, M. Pierantozzi, S. Tomassetti, and G. Coccia, Surface tension calculation from liquid viscosity data of silanes, *Fluid Phase Equil.* **463**, 11 (2018).
- [31] G. Sun, S. Saw, I. Douglas, and P. Harrowell, Structural origin of enhanced dynamics at the surface of a glassy alloy, *Phys. Rev. Lett.* **119**, 245501 (2017).
- [32] We use the “tensile” convention common in rheology, noting that some authors use a “compressive” convention with the opposite sign.
- [33] U. M. B. Marconi, C. Maggi, and S. Melchionna, Pressure and surface tension of an active simple liquid: a comparison between kinetic, mechanical and free-energy based approaches, *Soft Matter* **12**, 5727 (2016).
- [34] T. Speck, Stochastic thermodynamics for active matter, *EPL* **114**, 30006 (2016).
- [35] S. Naghieh and X. Chen, Printability—a key issue in extrusion-based bioprinting, *J. Pharmaceutical Analysis* **11**, 564 (2021).
- [36] S. Geisel, E. Secchi, and J. Vermant, Experimental challenges in determining the rheological properties of bacterial biofilms, *Interface Focus* **12**, 20220032 (2022).
- [37] S. G. V. Charlton, A. N. Bible, E. Secchi, J. L. Morrell-Falvey, S. T. Retterer, T. P. Curtis, J. Chen, and S. Jana, Microstructural and rheological transitions in bacterial biofilms, *Adv. Sci.* **10**, 2207373 (2023).